HHS Public Access

Author manuscript

*J Med Genet*. Author manuscript; available in PMC 2022 March 01.

Published in final edited form as:

*J Med Genet*. 2022 March ; 59(3): 294–304. doi:10.1136/jmedgenet-2020-107447.

# *DDX58(*RIG-I)-related disease is associated with tissue-specific interferon pathway activation

**Lev Prasov**[1,2,*], **Brenda L. Bohnsack**[1,3,4], **Antonette El Husny**[5], **Lam C. Tsoi**[6,7], **Bin Guan**[8], **J. Michelle Kahlenberg**[6,9], **Edmundo Almeida**[10], **Haitao Wang**[11], **Edward W. Cowen**[12], **Adriana A. De Jesus**[13], **Priyam Jani**[14], **Allison C. Billi**[6], **Sayoko E. Moroi**[1,15], **Rachael Wasikowski**[6], **Izabela Almeida**[16], **Luciana Almeida**[10], **Fernando Kok**[17], **Sarah J. Garnai**[1], **Shahzad I. Mian**[1], **Marcus Y. Chen**[18], **Blake M. Warner**[14], **Carlos R. Ferreira**[19], **Raphaela Goldbach-Mansky**[13], **Sun Hur**[11], **Brian P. Brooks**[8], **Julia E. Richards**[1,20], **Robert B. Hufnagel**[8], **Johann E. Gudjonsson**[6]

[1]Department of Ophthalmology and Visual Sciences, University of Michigan, Ann Arbor, MI, USA

[2]Department of Human Genetics, University of Michigan, Ann Arbor, MI, USA

[3]Division of Ophthalmology, Ann & Robert H. Lurie Children's Hospital of Chicago. Chicago, IL, USA

[4]Department of Ophthalmology, Northwestern University, Chicago, IL, USA 60611

[5]Children's and Adolescents' Health Care Unit, Bettina Ferro de Souza University Hospital, Federal University of Pará, Belém, PA, Brazil

[6]Department of Dermatology, University of Michigan Medical School, Ann Arbor, MI, USA

[7]Department of Computational Medicine & Bioinformatics, University of Michigan Medical School, Ann Arbor, Michigan, USA.

[8]Ophthalmic Genetics and Visual Function Branch, National Eye Institute, National Institutes of Health, Bethesda, MD

[9]Division of Rheumatology, Department of Internal Medicine, University of Michigan, Ann Arbor, MI, USA

[10]Department of Ophthalmology, Federal University of Pará, Belém, PA, Brazil

[11]Program in Cellular and Molecular Medicine, Boston Children's Hospital, Boston, MA, USA

[12]Dermatology Branch, National Institute of Arthritis and Musculoskeletal and Skin Diseases, National Institutes of Health, Bethesda, MD, USA

[13]Translational Autoinflammatory Disease Studies, National Institute of Allergy and Infectious Diseases, National Institutes of Health, Bethesda, MD, USA

[*]Author for correspondence: Lev Prasov, MD, PhD, 229 Kellogg Eye Center, 1000 Wall St. Ann Arbor, MI 48105, Tel 734-763-3732 lprasov@med.umich.edu.

COMPETING INTERESTS:
No competing interests.

[14]Craniofacial Anomalies and Regeneration Section, National Institute of Dental and Craniofacial Research, National Institutes of Health, Bethesda, MD, USA

[15]Department of Ophthalmology and Visual Sciences, The Ohio State University Wexner Medical Center, Columbus, OH, USA

[16]Department of Ophthalmology and Visual Sciences, Federal University of São Paulo, São Paulo, SP, Brazil

[17]Mendelics Genomic Analysis, São Paulo, SP, Brazil

[18]Cardiovascular Branch, National Heart, Lung and Blood Institute, National Institutes of Health, Bethesda, MD, USA

[19]Medical Genomics and Metabolic Genetics Branch, National Human Genome Research Institute, National Institutes of Health, Bethesda, MD 20892

[20]Department of Epidemiology, University of Michigan School of Public Health, Ann Arbor, MI, USA

## Abstract

**Background:** Singleton-Merten Syndrome (SGMRT) is a rare immunogenetic disorder that variably features juvenile open-angle glaucoma (JOAG), psoriasiform skin rash, aortic calcifications, and skeletal and dental dysplasia. Few families have been described and the genotypic and phenotypic spectrum is poorly defined, with variants in *DDX58* (DExD/H-box helicase 58) being one of two identified causes, classified as SGMRT2.

**Methods:** Families underwent deep systemic phenotyping and exome sequencing. Functional characterization with *in vitro* luciferase assays and *in vivo* interferon signature using bulk and single cell RNA sequencing was performed.

**Results:** We have identified a novel *DDX58* variant c.1529A>T p.(Glu510Val) that segregates with disease in two families with SGMRT2. Patients in these families have widely variable phenotypic features and different ethnic background, with some being severely affected by systemic features, and others solely with glaucoma. JOAG was present in all individuals affected with the syndrome. Furthermore, detailed evaluation of skin rash in one patient revealed sparse inflammatory infiltrates in a unique distribution. Functional analysis showed that the *DDX58* variant is a dominant gain-of-function activator of interferon pathways in the absence of exogenous RNA ligands. Single cell RNA sequencing of patient lesional skin revealed a cellular activation of interferon-stimulated gene expression in keratinocytes and fibroblasts but not in neighboring healthy skin.

**Conclusions:** These results expand the genotypic spectrum of DDX58-associated disease, provide the first detailed description of ocular and dermatologic phenotypes, expand our understanding of the molecular pathogenesis of this condition, and provide a platform for testing response to therapy.

### Keywords

Juvenile open-angle glaucoma; Pediatric glaucoma; interferon; DExD/H-box helicase 58; DDX58; RIG-I; Aortic calcification; Psoriasis; Singleton-Merten Syndrome; Tendon rupture

## INTRODUCTION

Singleton-Merten syndrome (SGMRT) is a rare multisystem genetic inflammatory disorder that variably features juvenile open angle glaucoma (JOAG), psoriasiform skin rash, vascular calcifications, dental anomalies, and skeletal dysplasia. *DDX58 (DExD/H-box helicase 58)* and *IFIH1 (interferon-induced with helicase C domain 1)* have been implicated in this condition causing SGMRT2 [MIM: 616298] and SGMRT1 [MIM: 182250], respectively.[1-6] Both genes encode proteins (RIG-I and MDA5, respectively) that recognize double-stranded RNA viruses and activate type I interferon pathways and proinflammatory cytokines, part of the innate immune response.[7,8] Identified variants in these genes have been dominant gain-of-function missense variants that activate interferon pathways in the absence of exogenous RNA ligands.[2-4]

*DDX58* and *IFIH1* are members of the retinoic acid inducible-like receptors (RLR) and recognize exogenous RNA from many viruses, including coronavirus, Zika virus, and rubella.[7,9-11] DDX58 signals downstream through the mitochondrial activating complex, ultimately activating TANK-binding kinase (TBK1).[8] In turn, downstream phosphorylation of IRF-3 and IRF-7 leads to transcriptional activation of interferon responsive genes and release of proinflammatory cytokines.[8,9]

Pathogenic variants in *DDX58* have been identified in two Korean and one Caucasian family with SGMRT2.[3,4] The phenotypic features of these families were quite variable, ranging from milder[4] to more severe.[3] JOAG has been seen in nearly all reported patients (12/13, 92%), and psoriasiform rash is also common (9/13, 69%). These features have been described in adult patients predominantly, so it is unclear when they develop and whether there are patients with only glaucoma or skin rash.

Here, we report two unrelated families with features of SGMRT who carry a novel *DDX58* variant. We use deep phenotyping to reveal novel aspects of this syndrome, including a detailed characterization of the ocular and skin features. Furthermore, through detailed functional characterization, we observe a tissue-specific activation of interferon responsive genes in lesional skin, suggesting organ systems may be variably affected.

## MATERIALS AND METHODS

### Human subjects and clinical testing

Human subjects work was approved by the Institutional Review Board (IRB) at the University of Michigan and National Institutes of Health. All subjects provided written informed consent for their inclusion and separate consent for publication. Brazilian subjects were consented in Portuguese, with data and images reviewed retrospectively, de-identified and exempt.

For Family A, clinical records were reviewed and blood samples processed for DNA extraction. Patients underwent standard clinical and surgical ophthalmic evaluation, which included best corrected visual acuity (BCVA), refraction, and slit-lamp and dilated fundus examination. Patients also had fundus color photography (Topcon, Tokyo, Japan;

Optos, Dunfermline, Scotland), spectral domain optical coherence tomography (Spectralis, Heidelberg, Germany), and static perimetry (Humphrey 24-2, Carl Zeiss Meditec, Dublin, CA, USA). Patients underwent systemic phenotyping including history and physical exam, computerized tomography (CT) scan, dental exam, and electrocardiogram. Dental evaluation included the occlusion, eruption pattern, tooth morphology, jaw relationship, and temporomandibular joint function, along with intra-oral photography (Canon EOS 5D Mark II camera, Canon USA Inc., Arlington, VA, USA) and 3-dimensional intraoral scans (3shape A/S, Copenhagen, Denmark). For Family B, systemic and ophthalmic records were reviewed, including imaging data, clinical, and surgical history.

## Genetic analysis

DNA from whole blood was extracted according to standard procedures as previously described.[12] For Family A exome sequencing, patient DNA samples were pooled equally based on dsDNA fluorescence quantification (QuantiFluor dsDNA System, Promega, Madison, WI, USA). One DNA pool was made for all known affected family members, and one for adult unaffected family members. Library preparation used the xGen Exome capture kit v1 (Integrated DNA Technologies, Coralville, Iowa, USA) and the Illumina NovaSeq Platform (San Diego, CA, USA) at the National Intramural Sequencing Center. Variants were called using a customized pipeline including MuTect2 in the Genome Analysis Toolkit,[13] using tumor (affected) / normal (unaffected) analysis (https://github.com/Bin-Guan/NGS_genotype_calling), and classified based on American College of Medical Genetics (ACMG) criteria.[14] The proband from Family B underwent clinical exome sequencing using Nextera Exome Capture (Illumina) followed Illumina HiSeq platform sequencing.

## Functional assays

Structural modeling in PyMOL (Schrödinger, LLC, New York, NY, USA) was based on human DDX58 (RIG-I) bound to dsRNA (PDB: 2ykg).[15] Sequence conservation was evaluated using Vertebrate MultiZ Alignment and Conservation[16] in the UC-Santa Cruz genome browser, with manual re-alignment of zebrafish *ddx58* (REFseq: NM_001306095.1).

Mutant FLAG-tagged RIG-I (DDX58) p.(Glu510Val) was constructed using site-directed mutagenesis starting from previously generated wild-type constructs (pFIag-CMV4-RIG-I) and using standard protocols.[3] Luciferase assays using HEK-293T cell transfected with wild-tpe and mutant DDX58 constructs along with *IFN*- promoter-driven firefly luciferase[17] in the presence or absence of RNA mimic 5AB were conducted as previously described.[3] Statistical analysis was done using two-tailed Student's *t*-test. Western blot analysis was done according to standard protocols with lysate preparation as done previously.[18] Primary antibodies were the following: mouse anti-FLAG M2-peroxidase (1:5000, Sigma-Aldrich, St. Louis, MO, USA) and rabbit anti-β-actin (1:5000, Cell Signaling, Danvers, MA, USA).

For Family A, interferon gene signature was determined from blood RNA from freshly collected patient samples as previously described.[3,19] Briefly, a standardized IFN score was calculated from gene expression analysis (Nanostring, Seattle, WA, USA) of 28 selected

interferon-stimulated genes (ISGs) normalized by subtracting the mean of healthy controls and dividing by the standard deviation of healthy controls.

### Bulk and single cell RNA (scRNA) sequencing

To generate single cell suspensions, lesional and nonlesional skin tissue was first obtained by punch biopsy from individual A-III-3. Sample processing, library preparation, and sequencing were performed as previously described[20] with the exception that all epidermal and dermal cells were pooled for sequencing. The samples were analyzed together with normal skin biopsy samples from 2 healthy Caucasian patients. Quality control, read alignment, and gene quantification was conducted using the 10X Genomics Cell Ranger software (Pleasanton, CA, USA). Seurat 3.0[21] was used for further normalization, data integration, and clustering analysis. Clustered cells were mapped to corresponding cell types by gene signatures as done previously[20]. Interferon response score was calculated using the same 28 ISG signature,[19] with z-score first computed for each gene in each cell, and the scores of the 28 genes averaged to compute the IFN score for each cell. Gene ontology (GO) term analysis was conducted in PANTHER[22]. Data processing and analysis for bulk RNA sequencing from lesional and non-lesional skin tissue from individual A-III-3 and A-IV-6, and healthy control skin, was done as previously described[23].

## RESULTS

### Clinical phenotypes of Singleton-Merten Syndrome families

The proband IV-6 from Family A (Figure 1A) of European descent presented at age three with severely elevated intraocular pressure (IOP). She underwent uncomplicated 360-degree trabeculotomy in both eyes and subsequently maintained normal IOP without glaucoma medications (Figure 2, Table 1). At age 11, her BCVA was 20/20 in each eye with no visual field loss, stable optic nerve appearance, and normal retinal nerve fiber layer thickness (Figure 2A-D). Systemically, she had history of prolonged QT interval on electrocardiogram (EKG). Dental examination revealed mixed dentition with delayed eruption pattern with 12 retained deciduous teeth at the time of examination (11 years old), along with severe crowding (Supplemental Figure 1). Additional evaluation with CT head, chest-abdomen, electrocardiogram, and history and physical examination evaluation by a medical geneticist did not reveal any abnormalities (Supplemental Figure 2-3). Individual A-IV-2, the proband's brother, presented at age 14 with abrupt onset of eye pain and blurred vision and was noted to have elevated IOP of 48 mmHg in the right eye and 39 mmHg in the left eye (Figure 2, Table 1). He underwent 360 trabeculotomy in the right eye, during which canalogram demonstrated minimal outflow downstream of Schlemm's Canal[25]. Hence, he underwent Baerveldt 350 glaucoma drainage device placement in the left eye. At age 19, his IOP was controlled on 4 classes of glaucoma medications in the right eye (timolol, dorzolamide, latanoprost, brimonidine) and 2 classes in the left eye (timolol and dorzolamide). He had preserved visual function and optic nerve structure, without significant progression of disease (Figure 2). Systemic phenotyping revealed joint subluxation of the left shoulder, and mild arthritic changes on hand and foot radiographs, but no vascular calcifications or intracranial calcifications, or bony anomalies (Supplemental Figure 2-3).

Dental exam revealed normal dentition with moderate enamel defects and mild crowding of mandibular anterior teeth (Supplemental Figure 1).

Individual A-III-3, father of proband, was diagnosed with JOAG at age 3 and underwent bilateral goniotomies followed by bilateral trabeculectomies with antifibrotics. He was subsequently stable on topical medications but developed bilateral corneal graft failure with band keratopathy and corneal neovascularization in his mid-20s. He underwent penetrating keratoplasty three times, with transplant failure after 18 months, then 4 years, then 10 years, and most recently Descemet Stripping Automated Endothelial Keratoplasty in his right eye (Figure 2E). He had no corneal surgeries in his left eye. BCVA at last exam was 20/40 in the right eye and light perception in the left eye. Fundus examination revealed severe optic disc cupping and pallor in the right eye with poor view due to corneal opacification in the left eye. Humphrey visual field showed severely constricted visual field in the right eye with dense superior and inferior arcuate defects (mean deviation: −17.94 dB, pattern standard deviation: 9.02 dB, Figure 2C-D). Systemically, the patient had intermittent arthritis symptoms beginning in college, which improved temporarily with azathioprine treatment. He also had spontaneous rupture of the Achilles tendon. CT of chest and abdomen demonstrated mild aortic calcifications and calcification of the proximal left subclavian artery, and iliac arteries (Figure 1B). External and radiographic evaluation of hands and feet were notable for periarticular calcification and bony erosion of the meta- and especially the proximal inter-phalangeal joints of the hands and feet (Figure 1C-E). Dental examination revealed normal appearance with restorations on multiple teeth (Supplemental Figure 1). C-reactive protein and Westergren sedimentation rate were normal. The patient developed a psoriasiform rash in his 20s on bilateral flanks, trunk, and extensor surfaces of the arms and legs that did not respond to topical steroid therapy and has continued to spread (Figure 3A-C). Histologic analysis of lesional skin showed psoriasiform epidermal hyperplasia with minimal infiltrate and absence of neutrophilic microabcesses (Figure 3D-E). Electrocardiogram was normal without evidence of arrythmia. Patient reported family history was notable for JOAG and blindness in the proband's paternal grandfather and great-grandfather, and her grandfather was also reported to have a skin rash and arthritis similar to individual A-III-3.

The proband from Family B (B-III-1) was of Brazilian native descent and first presented with glaucoma at age 5. At that time, his IOP was 38 mmHg bilaterally and cup-disc ratio was noted to be 0.8 in both eyes. He underwent urgent bilateral trabeculotomies. He developed bilateral corneal opacification at age 13 years secondary to corneal decompensation, and underwent penetrating keratoplasty in each eye. Due to graft failure and rejection over the next several years, he subsequently had two additional penetrating keratoplasties in each eye. He suffered a blunt trauma in the left eye at age 14, with resulting corneal graft dehiscence, lens dislocation and retinal detachment. At age 21 years, he underwent placement of an Ahmed-FP7 glaucoma tube in left eye, but the eye became hypotonous and developed phthisis bulbi over several years. At his last examination at age 31, the patient's BCVA was 20/100 in the right eye and no light perception in the left eye, and IOP was 8 mmHg and 0 mmHg, respectively. Anterior segment exam demonstrated a failing corneal transplant with band keratopathy and peripheral corneal neovascularization in the right eye (Figure 2F) and phthisis bulbi of the left eye. Systemic phenotyping revealed

hypoplastic distal second digits (Figure 1G-I), mild finger-nail dysplasia and severe toenail hypoplasia (Figure 1G-I). He was noted to have brittle teeth, caries and gingivitis from age 8 and developed a recurrent psoriasiform skin rash at age 12. He also developed arthralgia at age 13 and had spontaneous Achilles tendon rupture bilaterally. Radiographs were notable for lumbosacral transitional vertebra, osteophytosis on patellofemoral and tibiofemoral joints, as well as calcaneus irregularities. Echocardiogram revealed mitral and aortic valve calcifications and left ventricular hypertrophy. The patient was diagnosed with cardiac arrythmia by age 24 and succumbed to heart failure and cardiogenic shock at age 32. The proband's sister (B-III-2) was diagnosed with glaucoma at age 8 and her last cardiac assessment revealed numerous premature ventricular contractions. Family history per report was notable for an autosomal dominant pattern of glaucoma, cardiomyopathy and dystrophic nails.

## Genetic analysis

Family A underwent pooled exome sequencing, which identified a missense variant in *DDX58* (RefSeq transcript ID: NM_014314.3) c.1529A>T p.(Glu510Val) and no other compelling variants (Figure 4). This variant segregated perfectly in all affected individuals and was absent from the unaffected pool (A-III-2 and A-III-4) or from unaffected individuals undergoing clinical diagnostic testing (Figure 4B). The proband in Family B had clinical exome sequencing, which revealed the same *DDX58* variant (ClinVar submission: SCV001137792.1). DDX58 Glu510 is highly conserved in vertebrate species and within the Hel-2i domain that contacts dsRNA ligands (Figure 4C-D). Structural modeling revealed that this residue makes a charge-charge contact with Arg546, which is disrupted with the valine substitution. The p.(Glu510Val) variant is absent in gnomAD (in over 240,000 alleles), predicted to be damaging by 15 *in silico* predictors[26] with a high genomic evolutionary rate profiling (GERP) score (5.05)[27] and high combined annotation dependent depletion (CADD) score (29.7),[28] and meets ACMG criteria[29] for being likely pathogenic (Supplemental Table 1).

## Functional analysis

To date, identified pathogenic variants in DDX58 associated with Singleton-Merten syndrome have been dominant gain-of-function variants that activate IFN pathways in the absence of an RNA ligand.[3,4] We used a validated IFN-b luciferase reporter assay in HEK-293T cells, comparing p.(Glu510Val) to previously reported variants p.(Cys268Phe) and p.(Gln517His).[3,4,17] There was significant basal activation of the reporter with *DDX58* p.(Glu510Val) as compared to wild-type ($p<0.05$), similar to that observed for the other two variants (Figure 4E). There were comparable levels of transfection/protein expression and all constructs showed further reporter activation in the presence of 5AB, an RNA mimic.

To further define the pattern of interferon stimulation, blood samples from affected and unaffected members of family A were subjected to validated Nanostring interferon signature analysis, and compared to previously generated controls from other inflammatory conditions (Neonatal onset multisystem inflammatory disease [NOMID], Chronic Atypical Neutrophilic Dermatosis with Lipodystrophy and Elevated Temperature [CANDLE], STING-associated vasculopathy with onset in infancy [SAVI]).[19] All family members had

negative interferon scores, similar to healthy controls, with no correlation between interferon score and disease activity (Figure 4F).

### Skin transcriptomic analysis

Given the unusual histologic features of the psoriasiform rash and the lack of elevated interferon scores in blood, we next used bulk and single cell RNA sequencing to establish a cellular and molecular signature for this condition. Single cells from lesional and adjacent unaffected skin from individual A-III-3 (Figure 3) were dissociated and underwent scRNA sequencing, and results were compared to those from previously collected healthy Caucasian controls. We collected 5,115 and 6,660 cells in the lesional and non-lesional skin, respectively, with a median of ~2,000 genes per cell. We performed unsupervised clustering analysis and grouped the cells into 13 clusters (Figure 5A), including keratinocytes (basal, differentiated and keratinized), fibroblasts, eccrine cells, endothelial cells, myeloid cells, mast cells, and T cells. The proportion between different cell types was fairly consistent between the three groups, with the exception of slight expansion of basal and differentiated keratinocytes, defined by the cluster having expression of *KRT14/MT2A/ASS1/WNT10A* and *KRT10/PTGS1/KTR6B/KRT1*, respectively[20] (Figure 5B). This was consistent with expansion of the epidermal compartment and the resultant psoriasis-like hyperplasia (Figure 3E). Interestingly, *DDX58* mRNA expression was increased in all three compartments of keratinocytes from inflamed skin compared to control skin (Figure 5C), consistent with *DDX58* serving as an ISG.[30] Similarly, *DDX58* expression was elevated in inflamed skin for fibroblasts and endothelial cells but not mast cells (Figure 5C). Consistent with this observation we found heightened IFN response score (Figure 5D; defined using 28 gene signature: Figure 5E)[19] in lesional fibroblasts and interfollicular epidermal cells compared to these populations in healthy control skin, but lower IFN score in non-lesional skin. These results were confirmed in bulk RNA sequencing analysis from individual A-III-3 and A-IV-2 (Supplemental Figure 4), though with comparable ISG expression in non-lesional and control skin. Surprisingly, *IFNA1* and *IFNB1* were not detected in lesional or non-lesional samples, though *IFNG* expression was elevated in T cells in lesional skin, possibly related to the long duration of disease activity in this individual (Supplemental Figure 5). In the lesional keratinocytes (differentiated) functional enrichment GO terms included “response to type I interferon” (false discovery rate [FDR] = $1.67x10^{-7}$), “innate immune response” (FDR = $6.59\ x10^{-6}$), and “programmed cell death” (FDR = 4.92E-4) (Supplemental Table 2). Consistent with the reduced IFN response signature we observed in non-lesional skin (Figure 5D), GO terms decreased in this population also included “response to type I interferon” (FDR = 4.47x1 $O^{-2}$, Supplemental Table 3), but less significantly so. Further, the average expression of IFN response genes was much higher in inflamed lesional skin from the patient (Supplemental Figure 4) than the baseline IFN response in control cells.

## DISCUSSION

Here, we have identified a novel gain-of-function variant in *DDX58* in two families with Singleton-Merten Syndrome Type 2, and have provided a very complete ocular, dermatologic, and molecular description of this rare syndrome with wide ranging implications for the innate immune system.

## Phenotypic variability of *DDX58*-associated disease

We have described two families with the same DDX58 p.(Glu510Val) variant leading to a very broad spectrum of ocular and systemic phenotypes (Figure 1-3). This spectrum of phenotypic features is consistent with prior reports, and suggest different features from *IFIH1*-associated disease.[4,31 32] None of the identified *DDX58* patients have significant neurologic findings or intracranial calcifications (Supplemental Figure 3),[3,4] to suggest overlap with the Aicardi-Goutieres spectrum as in *IFIH1* disease.[32] Additionally, glaucoma is the most penetrant feature of *DDX58*-related disease (Table 1), and blood interferon signature is variable (Figure 4),[3] unlike *IFIHI*-related disorder.[2] Though glaucoma is common to nearly all of the described family members, the age at diagnosis and the severity is variable. These results suggest that other exogenous factors such as genetic predispositions at other loci or environmental triggers may contribute to disease pathogenesis. Intriguingly, DDX58 plays an important role in pathogen recognition for double-stranded RNA viruses, such as Zika virus and rubella virus.[10,11] Infection with these viruses has been associated with a high rate of infantile-onset glaucoma,[33,34] suggesting a possibility that DDX58 could contribute to disease pathogenesis in these infections.

There is striking phenotypic variability also for systemic phenotypes. The two adult individuals in United States and Brazilian families have the same genotype, but varying severity and tissue involvement. Individual A-III-3 has psoriasiform rash and significant joint calcifications, but very mild aortic involvement and no nail changes (Figure 1B-E). Individual B-III-1 has severe aortic calcifications and nail hypoplasia, but lacks joint calcifications (Figure 1F-I). Thus, the pleiotropic effects are not clearly driven by the genotype. Additionally, variants that have a lower level of basal interferon activation *in vitro* (i.e. p.Gln517His) can lead to more severe systemic phenotypes.[3]

Some younger individuals in our study have isolated JOAG and none of the other systemic features. As such, it remains possible that *DDX58* or environmental triggers of this pathway explain a much larger proportion of JOAG patients than previously thought. As some JOAG cases may be pre-symptomatic for the other systemic features of SGMRT2, as evidenced by individual A-IV-2, diligent screening for systemic features is necessary, given that cardiac calcifications are a frequent cause of mortality in these patients. Some individuals show evidence only of glaucoma (i.e. A-IV-6). Others may not show any features until later in life, supporting the value of genetic testing and counseling in these unaffected family members.

Interestingly, the most severely affected individuals from both families had significant conjunctival calcifications and suffered early corneal graft failure. While the presence of glaucoma is a risk factor for corneal graft failure[35,36] and penetrating keratoplasty may exacerbate glaucoma,[37] immune mechanisms may also be involved. Indeed, treatment with alpha-2 interferon has been associated with development of graft rejection,[38] and this pathway is activated in SGMRT.[8]

## Novel skin features of this disorder

We have provided the first comprehensive description of the skin findings of an individual with SGMRT2, with detailed gross, histologic, and gene expression analysis. Interestingly,

the skin rash of SGMRT2 shows increased cornification and epidermal hyperplasia, however, in contrast to psoriasis and cutaneous lupus, inflammatory infiltrates were sparse. While *DDX58* expression was predominantly in tissue resident cells, the lack of ISG expression in non-lesional skin, and the prominent *IFNG* expression, along with absence of other type I IFNs in lesional skin, suggest involvement of the adaptive immunity for full development of the inflammatory skin phenotype. The distinct presentation of the skin rash involved both the trunk and extremities, demonstrated fine scale, lacked sharp demarcation from normal skin. Given that this is one of the most consistent features of the syndrome (together with glaucoma), the skin may be the most amenable for monitoring disease activity and response to treatment.

## Tissue specificity in interferon activation

We have defined a novel gain-of-function DDX58 p.(Glu510Val) variant that activates ISG expression. We have shown that *in vitro* this variant activates interferon pathways to a basal low level in the absence of an RNA ligand. Evaluating the blood interferon signature and cutaneous scRNA sequencing data from Family A, we have uncovered a striking cell type and tissue specific response. In a previously assessed family, the interferon score was elevated in the proband, but not the older family member.[3] However, family A members have a negative blood standardized interferon score, which is below the score for many healthy control individuals. Individual A-III-3 clearly has disease activity as evidenced by his active skin lesions and arthralgia. Consistent with this, ISGs were upregulated in lesional skin among many of the cell types, but not in neighboring healthy skin. DDX58 is most prominently expressed in keratinized and differentiated epithelium, which shows the strongest ISG response. These results could be explained by the fact that mutant DDX58 exerts a cell and tissue specific response, guided by a unique endogenous and exogenous RNA environment in different cells and tissues. Indeed, differential recognition of endogenous RNAs (Alu duplexes) leading to activation of downstream signaling was observed with Aicardi-Goutieres associated variants of *IFIH1* (MDA5),[18] suggesting this could be a pathogenic mechanism for RIG-I-like receptor mutations. The interferon suppression in non-lesional skin could be the result of homeostatic mechanisms to limit basal interferon signature or differential response to stress, but this remains to be evaluated experimentally. Alternatively, variability in basal interferon activity may be influenced by other genetic or environmental factors leading to variability among patients and populations. For instance, keratinocytes in the skin have constant interaction with the microbial and viral world, which may lead to tonic stimulation of DDX58/RIG-I signaling.

While there is a clear role of the immune system in glaucoma,[39] specific molecular mechanisms remain poorly defined. The discovery of a novel immunogenetic syndrome, with systemic features in accessible tissues such as the skin, allows for further characterization of the role of the immune system in glaucoma pathogenesis. Given that DDX58 functions as an environmental sensor, these discoveries also suggest a possible role for innate immune mechanisms in more common forms of glaucoma. Furthermore, our studies provide a framework for using gene expression analysis from the skin to develop targeted therapies for this condition.

## Supplementary Material

Refer to Web version on PubMed Central for supplementary material.

## ACKNOWLEDGEMENTS

The authors are grateful to the patients and families for participating in the study; to the NIH Intramural Sequencing Center for conducting pooled exome sequencing; to David McGaughey and the NEI Bioinformatics group for sequencing pipeline development; to Sally Camper for helpful discussions; to Xin Mu, Cara Lwin, and Amelia Naik for technical assistance.

FUNDING

The NEI K12 EY022299 (L.P.) and NEI P30 EY07003 (L.P.). NEI intramural funds (R.B.H, B.G., B.P.B). The National Institute of Arthritis and Musculoskeletal and Skin Diseases of the National Institutes of Health R01-AR060802 (J.E.G.), P30-AR075043 (J.E.G.), and K01-AR072129 (L.C.T.), and the National Institute of Allergy and Infectious Diseases under R01-AR069071 (J.E.G.), the A. Alfred Taubman Medical Research Institute (J.E.G. and J.M.K.) and the Parfet Emerging Scholar Award (J.M.K.).

## DATA AVAILABILITY STATEMENT

All underlying data are available upon reasonable request from the corresponding author or the study team.

## REFERENCES:

1. Singleton EB, Merten DF. An unusual syndrome of widened medullary cavities of the metacarpals and phalanges, aortic calcification and abnormal dentition. Pediatr Radiol 1973;1(1):2–7 doi: 10.1007/BF00972817published Online First: Epub Date]|. [PubMed: 4272099]
2. Rutsch F, MacDougall M, Lu C, Buers I, Mamaeva O, Nitschke Y, Rice GI, Erlandsen H, Kehl HG, Thiele H, Nurnberg P, Hohne W, Crow YJ, Feigenbaum A, Hennekam RC. A specific IFIH1 gain-of-function mutation causes Singleton-Merten syndrome. American journal of human genetics 2015;96(2):275–82 doi: 10.1016/j.ajhg.2014.12.014published Online First: Epub Date]|. [PubMed: 25620204]
3. Ferreira CR, Crow YJ, Gahl WA, Gardner PJ, Goldbach-Mansky R, Hur S, de Jesus AA, Nehrebecky M, Park JW, Briggs TA. DDX58 and Classic Singleton-Merten Syndrome. Journal of clinical immunology 2019;39(1):75–80 doi: 10.1007/s10875-018-0572-1published Online First: Epub Date]|. [PubMed: 30574673]
4. Jang MA, Kim EK, Now H, Nguyen NT, Kim WJ, Yoo JY, Lee J, Jeong YM, Kim CH, Kim OH, Sohn S, Nam SH, Hong Y, Lee YS, Chang SA, Jang SY, Kim JW, Lee MS, Lim SY, Sung KS, Park KT, Kim BJ, Lee JH, Kim DK, Kee C, Ki CS. Mutations in DDX58, which encodes RIG-I, cause atypical Singleton-Merten syndrome. American journal of human genetics 2015;96(2):266–74 doi: 10.1016/j.ajhg.2014.11.019published Online First: Epub Date]|. [PubMed: 25620203]
5. Feigenbaum A, Muller C, Yale C, Kleinheinz J, Jezewski P, Kehl Hg, MacDougall M, Rutsch F, Hennekam RC. Singleton-Merten syndrome: an autosomal dominant disorder with variable expression. Am J Med Genet A 2013;161A(2):360–70 doi: 10.1002/ajmg.a.35732published Online First: Epub Date]|. [PubMed: 23322711]
6. Gay BB Jr., Kuhn JP. A syndrome of widened medullary cavities of bone, aortic calcification, abnormal dentition, and muscular weakness (the Singleton-Merten syndrome). Radiology 1976;118(2):389–95 doi: 10.1148/118.2.389published Online First: Epub Date]|. [PubMed: 175395]
7. Kell AM, Gale M Jr. RIG-I in RNA virus recognition. Virology 2015;479-480:110–21 doi: 10.1016/j.virol.2015.02.017published Online First: Epub Date]|. [PubMed: 25749629]
8. Lu C, MacDougall M. RIG-I-Like Receptor Signaling in Singleton-Merten Syndrome. Front Genet 2017;8:118 doi: 10.3389/fgene.2017.00118published Online First: Epub Date]|. [PubMed: 28955379]

9. Brisse M, Ly H. Comparative Structure and Function Analysis of the RIG-I-Like Receptors: RIG-I and MDA5. Front Immunol 2019;10:1586 doi: 10.3389/fimmu.2019.01586published Online First: Epub Date]|. [PubMed: 31379819]
10. Ovsyannikova IG, Dhiman N, Haralambieva IH, Vierkant RA, O'Byrne MM, Jacobson RM, Poland GA. Rubella vaccine-induced cellular immunity: evidence of associations with polymorphisms in the Toll-like, vitamin A and D receptors, and innate immune response genes. Hum Genet 2010;127(2):207–21 doi: 10.1007/s00439-009-0763-1published Online First: Epub Date]|. [PubMed: 19902255]
11. Chazal M, Beauclair G, Gracias S, Najburg V, Simon-Loriere E, Tangy F, Komarova AV, Jouvenet N. RIG-I Recognizes the 5' Region of Dengue and Zika Virus Genomes. Cell Rep 2018;24(2):320–28 doi: 10.1016/j.celrep.2018.06.047published Online First: Epub Date]|. [PubMed: 29996094]
12. Garnai SJ, Brinkmeier ML, Emery B, Aleman TS, Pyle LC, Veleva-Rotse B, Sisk RA, Rozsa FW, Ozel AB, Li JZ, Moroi SE, Archer SM, Lin CM, Sheskey S, Wiinikka-Buesser L, Eadie J, Urquhart JE, Black GCM, Othman MI, Boehnke M, Sullivan SA, Skuta GL, Pawar HS, Katz AE, Huryn LA, Hufnagel RB, Genomic Ascertainment C, Camper SA, Richards JE, Prasov L. Variants in myelin regulatory factor (MYRF) cause autosomal dominant and syndromic nanophthalmos in humans and retinal degeneration in mice. PLoS genetics 2019;15(5):e1008130 doi: 10.1371/journal.pgen.1008130published Online First: Epub Date]|. [PubMed: 31048900]
13. Benjamin D, Sato T, Cibulskis K, Getz G, Stewart C, Lichtenstein L. Calling Somatic SNVs and Indels with Mutect2. bioRxiv 2019:861054 doi: 10.1101/861054published Online First: Epub Date]|.
14. Richards S, Aziz N, Bale S, Bick D, Das S, Gastier-Foster J, Grody WW, Hegde M, Lyon E, Spector E, Voelkerding K, Rehm HL, Committee ALQA. Standards and guidelines for the interpretation of sequence variants: a joint consensus recommendation of the American College of Medical Genetics and Genomics and the Association for Molecular Pathology. Genetics in medicine : official journal of the American College of Medical Genetics 2015;17(5):405–24 doi: 10.1038/gim.2015.30published Online First: Epub Date]|. [PubMed: 25741868]
15. Luo D, Kohlway A, Vela A, Pyle AM. Visualizing the determinants of viral RNA recognition by innate immune sensor RIG-I. Structure 2012;20(11):1983–8 doi: 10.1016/j.str.2012.08.029published Online First: Epub Date]|. [PubMed: 23022350]
16. Blanchette M, Kent WJ, Riemer C, Elnitski L, Smit AF, Roskin KM, Baertsch R, Rosenbloom K, Clawson H, Green ED, Haussler D, Miller W. Aligning multiple genomic sequences with the threaded blockset aligner. Genome Res 2004;14(4):708–15 doi: 10.1101/gr.1933104published Online First: Epub Date]|. [PubMed: 15060014]
17. Peisley A, Wu B, Xu H, Chen ZJ, Hur S. Structural basis for ubiquitin-mediated antiviral signal activation by RIG-I. Nature 2014;509(7498):110–4 doi: 10.1038/nature13140published Online First: Epub Date]|. [PubMed: 24590070]
18. Ahmad S, Mu X, Yang F, Greenwald E, Park JW, Jacob E, Zhang CZ, Hur S. Breaching Self-Tolerance to Alu Duplex RNA Underlies MDA5-Mediated Inflammation. Cell 2018;172(4):797–810 e13 doi: 10.1016/j.cell.2017.12.016published Online First: Epub Date]|. [PubMed: 29395326]
19. Kim H, de Jesus AA, Brooks SR, Liu Y, Huang Y, VanTries R, Montealegre Sanchez GA, Rotman Y, Gadina M, Goldbach-Mansky R. Development of a Validated Interferon Score Using NanoString Technology. J Interferon Cytokine Res 2018;38(4):171–85 doi: 10.1089/jir.2017.0127published Online First: Epub Date]|. [PubMed: 29638206]
20. Tsoi LC, Gharaee-Kermani M, Berthier CC, Nault T, Hile GA, Estadt SN, Patrick MT, Wasikowski R, Billi AC, Lowe L, Reed TJ, Gudjonsson JE, Kahlenberg JM. IL18-containing 5-gene signature distinguishes histologically identical dermatomyositis and lupus erythematosus skin lesions. JCI Insight 2020;5(16) doi: 10.1172/jci.insight.139558published Online First: Epub Date]|.
21. Butler A, Hoffman P, Smibert P, Papalexi E, Satija R. Integrating single-cell transcriptomic data across different conditions, technologies, and species. Nat Biotechnol 2018;36(5):411–20 doi: 10.1038/nbt.4096published Online First: Epub Date]|. [PubMed: 29608179]
22. Mi H, Muruganujan A, Ebert D, Huang X, Thomas PD. PANTHER version 14: more genomes, a new PANTHER GO-slim and improvements in enrichment analysis tools. Nucleic Acids Res 2019;47(D1):D419–D26 doi: 10.1093/nar/gky1038published Online First: Epub Date]|. [PubMed: 30407594]

23. Gudjonsson JE, Tsoi LC, Ma F, Billi AC, van Straalen KR, Vossen A, van der Zee HH, Harms PW, Wasikowski R, Yee CM, Rizvi SM, Xing X, Xing E, Plazyo O, Zeng C, Patrick MT, Lowe MM, Burney RE, Kozlow JH, Cherry-Bukowiec JR, Jiang Y, Kirma J, Weidinger S, Cushing KC, Rosenblum MD, Berthier C, MacLeod AS, Voorhees JJ, Wen F, Kahlenberg JM, Maverakis E, Modlin RL, Prens EP. Contribution of plasma cells and B cells to hidradenitis suppurativa pathogenesis. JCI Insight 2020;5(19) doi: 10.1172/jci.insight.139930published Online First: Epub Date]|.

24. de Carvalho LM, Ngoumou G, Park JW, Ehmke N, Deigendesch N, Kitabayashi N, Melki I, Souza FFL, Tzschach A, Nogueira-Barbosa MH, Ferriani V, Louzada-Junior P, Marques W Jr., Lourenco CM, Horn D, Kallinich T, Stenzel W, Hur S, Rice GI, Crow YJ. Musculoskeletal Disease in MDA5-Related Type I Interferonopathy: A Mendelian Mimic of Jaccoud's Arthropathy. Arthritis Rheumatol 2017;69(10):2081–91 doi: 10.1002/art.40179published Online First: Epub Date]|. [PubMed: 28605144]

25. Moroi SE, Reed DM, Sanders DS, Almazroa A, Kagemann L, Shah N, Shekhawat N, Richards JE. Precision medicine to prevent glaucoma-related blindness. Current opinion in ophthalmology 2019;30(3):187–98 doi: 10.1097/ICU.0000000000000564published Online First: Epub Date]|. [PubMed: 30883441]

26. Kopanos C, Tsiolkas V, Kouris A, Chapple CE, Albarca Aguilera M, Meyer R, Massouras A. VarSome: the human genomic variant search engine. Bioinformatics 2019;35(11): 1978–80 doi: 10.1093/bioinformatics/bty897published Online First: Epub Date]|. [PubMed: 30376034]

27. Davydov EV, Goode DL, Sirota M, Cooper GM, Sidow A, Batzoglou S. Identifying a high fraction of the human genome to be under selective constraint using GERP++. PLoS computational biology 2010;6(12):e1001025 doi: 10.1371/journal.pcbi.1001025published Online First: Epub Date]|. [PubMed: 21152010]

28. Rentzsch P, Witten D, Cooper GM, Shendure J, Kircher M. CADD: predicting the deleteriousness of variants throughout the human genome. Nucleic Acids Res 2019;47(D1):D886–D94 doi: 10.1093/nar/gky1016published Online First: Epub Date]|. [PubMed: 30371827]

29. Li Q, Wang K. InterVar: Clinical Interpretation of Genetic Variants by the 2015 ACMG-AMP Guidelines. American journal of human genetics 2017;100(2):267–80 doi: 10.1016/j.ajhg.2017.01.004published Online First: Epub Date]|. [PubMed: 28132688]

30. Matsumiya T, Stafforini DM. Function and regulation of retinoic acid-inducible gene-I. Crit Rev Immunol 2010;30(6):489–513 doi: 10.1615/critrevimmunol.v30.i6.10published Online First: Epub Date]|. [PubMed: 21175414]

31. Rice GI, Del Toro Duany Y, Jenkinson EM, Forte GM, Anderson BH, Ariaudo G, Bader-Meunier B, Baildam EM, Battini R, Beresford MW, Casarano M, Chouchane M, Cimaz R, Collins AE, Cordeiro NJ, Dale RC, Davidson JE, De Waele L, Desguerre I, Faivre L, Fazzi E, Isidor B, Lagae L, Latchman AR, Lebon P, Li C, Livingston JH, Lourenco CM, Mancardi MM, Masurel-Paulet A, McInnes IB, Menezes MP, Mignot C, O'Sullivan J, Orcesi S, Picco PP, Riva E, Robinson RA, Rodriguez D, Salvatici E, Scott C, Szybowska M, Tolmie JL, Vanderver A, Vanhulle C, Vieira JP, Webb K, Whitney RN, Williams SG, Wolfe LA, Zuberi SM, Hur S, Crow YJ. Gain-of-function mutations in IFIH1 cause a spectrum of human disease phenotypes associated with upregulated type I interferon signaling. Nature genetics 2014;46(5):503–09 doi: 10.1038/ng.2933published Online First: Epub Date]|. [PubMed: 24686847]

32. Rice GI, Park S, Gavazzi F, Adang LA, Ayuk LA, Van Eyck L, Seabra L, Barrea C, Battini R, Belot A, Berg S, Billette de Villemeur T, Bley AE, Blumkin L, Boespflug-Tanguy O, Briggs TA, Brimble E, Dale RC, Darin N, Debray FG, De Giorgis V, Denecke J, Doummar D, Drake Af Hagelsrum G, Eleftheriou D, Estienne M, Fazzi E, Feillet F, Galli J, Hartog N, Harvengt J, Heron B, Heron D, Kelly DA, Lev D, Levrat V, Livingston JH, Marti I, Mignot C, Mochel F, Nougues MC, Oppermann I, Perez-Duenas B, Popp B, Rodero MP, Rodriguez D, Saletti V, Sharpe C, Tonduti D, Vadlamani G, Van Haren K, Tomas Vila M, Vogt J, Wassmer E, Wiedemann A, Wilson CJ, Zerem A, Zweier C, Zuberi SM, Orcesi S, Vanderver AL, Hur S, Crow YJ. Genetic and phenotypic spectrum associated with IFIH1 gain-of-function. Human mutation 2020;41(4):837–49 doi: 10.1002/humu.23975published Online First: Epub Date]|. [PubMed: 31898846]

33. Yepez JB, Murati FA, Pettito M, Penaranda CF, de Yepez J, Maestre G, Arevalo JF, Johns Hopkins Zika C. Ophthalmic Manifestations of Congenital Zika Syndrome in Colombia and Venezuela.

JAMA Ophthalmol 2017;135(5):440–45 doi: 10.1001/jamaophthalmol.2017.0561published Online First: Epub Date]|. [PubMed: 28418539]

34. O'Neill JF. The ocular manifestations of congenital infection: a study of the early effect and long-term outcome of maternally transmitted rubella and toxoplasmosis. Trans Am Ophthalmol Soc 1998;96:813–79 [PubMed: 10360309]
35. Price MO, Thompson RW Jr., Price FW Jr. Risk factors for various causes of failure in initial corneal grafts. Archives of ophthalmology 2003; 121 (8): 1087–92 doi: 10.1001/archopht.121.8.1087published Online First: Epub Date]|. [PubMed: 12912684]
36. Anshu A, Price MO, Price FW. Descemet's stripping endothelial keratoplasty: long-term graft survival and risk factors for failure in eyes with preexisting glaucoma. Ophthalmology 2012;119(10):1982–7 doi: 10.1016/j.ophtha.2012.04.031published Online First: Epub Date]|. [PubMed: 22705345]
37. Haddadin RI, Chodosh J. Corneal transplantation and glaucoma. Semin Ophthalmol 2014;29(5-6):380–96 doi: 10.3109/08820538.2014.959201published Online First: Epub Date]|. [PubMed: 25325864]
38. Jacobs AD, Levenson JE, Golde DW. Induction of acute corneal allograft rejection by alpha-2 interferon. Am J Med 1987;82(1):181–2 doi: 10.1016/0002-9343(87)90405-0published Online First: Epub Date]|. [PubMed: 3541600]
39. Kamat SS, Gregory MS, Pasquale LR. The Role of the Immune System in Glaucoma: Bridging the Divide Between Immune Mechanisms in Experimental Glaucoma and the Human Disease. Semin Ophthalmol 2016;31(1-2):147–54 doi: 10.3109/08820538.2015.1114858published Online First: Epub Date]|. [PubMed: 26959140]

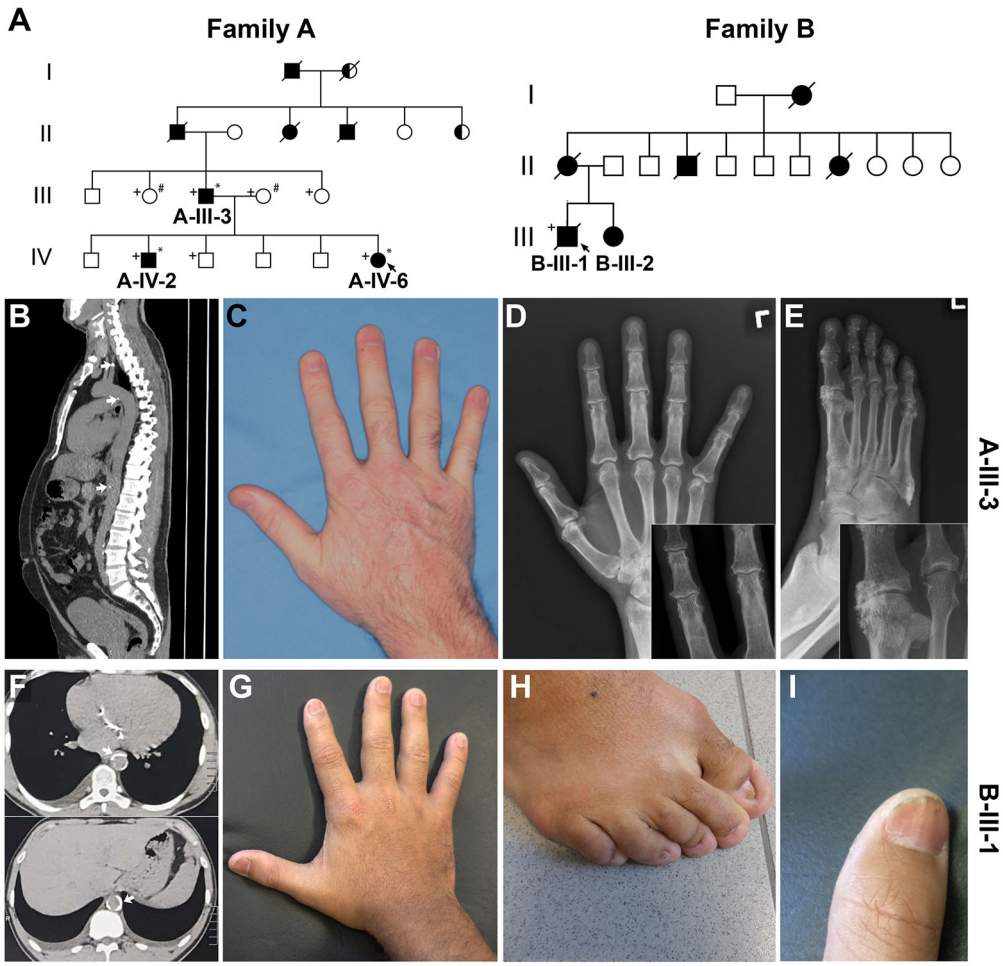


**Figure 1.**

Systemic findings in two families with Singleton-Merten syndrome. (A) Pedigrees of SGMRT2 families. Shaded individuals are affected with pediatric onset glaucoma and variably with other features of SGMRT2. Half-shaded individuals have adult onset open angle glaucoma. (B-E) Clinical features of individual A-III-3, including CT scan (B) showing aortic and large vessel calcifications (arrows), external hand photo showing joint swelling (C), hand (D) and foot (E) radiographs showing joint calcifications. (F-I) Clinical features of individual B-III-1, including chest CT showing aortic calcifications (F), external photo of hand (G), foot (H), and finger (I) showing clinodactyly, nail hypoplasia, and distal phalangeal hypoplasia. +, sampled individuals; *, included for affected pooled exome; #, included for unaffected pool.

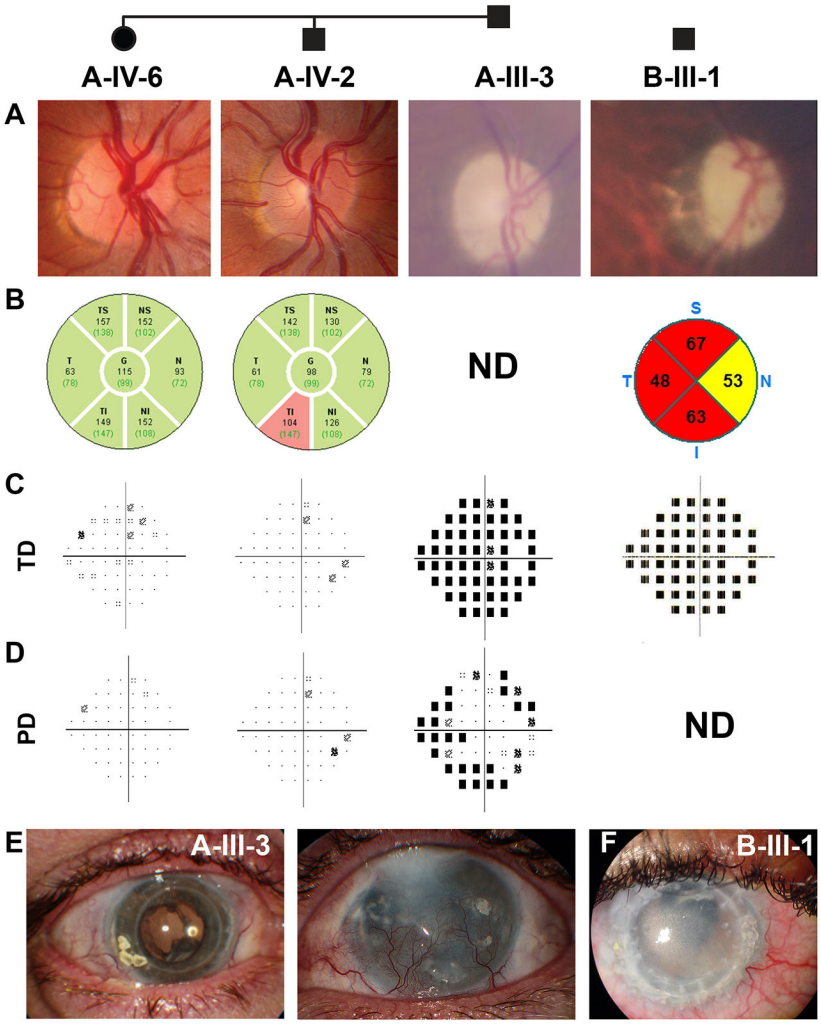


**Figure 2.**

Ocular findings in Singleton-Merten syndrome. (A-D) Ophthalmic imaging and testing from right eyes of SGMRT2 patients including optic disc photos (A) of affected patients from two families (family A, left; family B, right), retinal nerve fiber layer thickness maps (B), Humphrey visual field 24-2 total deviation (C) and pattern deviation (D) maps. (E) External photo of right and left eyes of individual A-III-3 showing calcium deposits on the cornea and corneal graft (left), corneal neovascularization and opacity (right). (F) External photo of the right eye of individual B-III-1 showed opacified corneal transplant with neovascularization.

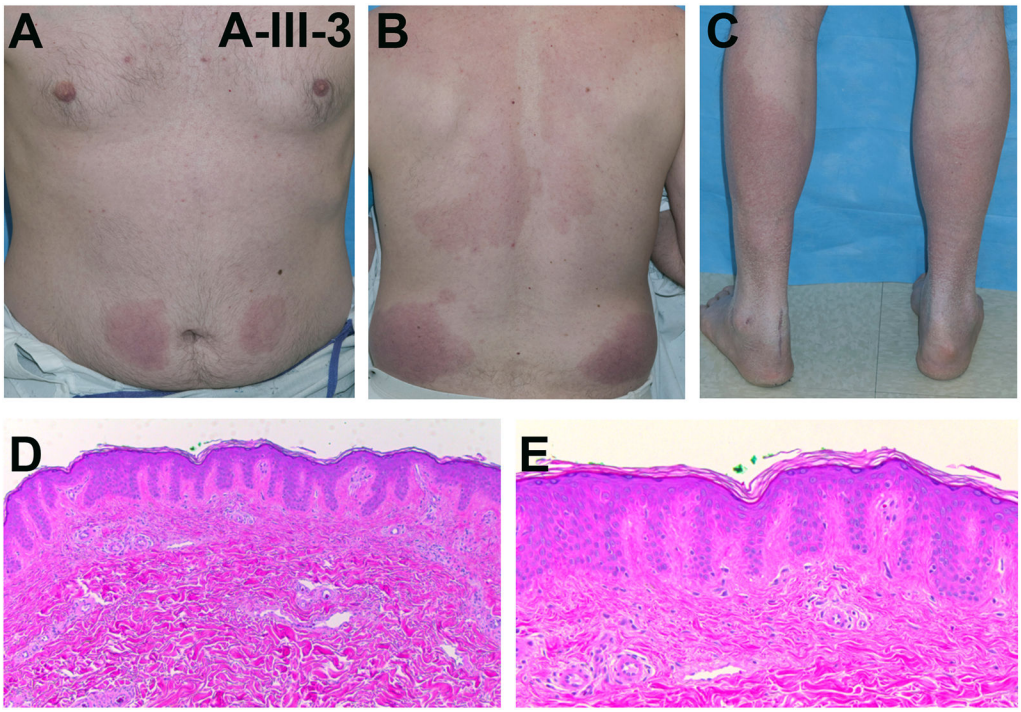


**Figure 3.**

Skin findings in Singleton-Merten syndrome. **(A-C)** External photos of A-III-3. Stable, thin pink scaling non-pruritic plaques symmetrically distributed on the abdomen (A), back (B) and extremities (C). (**D-E**) Histologic findings in skin eruption of Singleton-Merten syndrome. Psoriasiform epidermal hyperplasia is noted, but there is minimal epidermal and dermal inflammatory infiltrate, and the neutrophilic micro-abscesses characteristic of psoriasis are notably absent (hematoxylin and eosin; d, 50x; e, 100x).

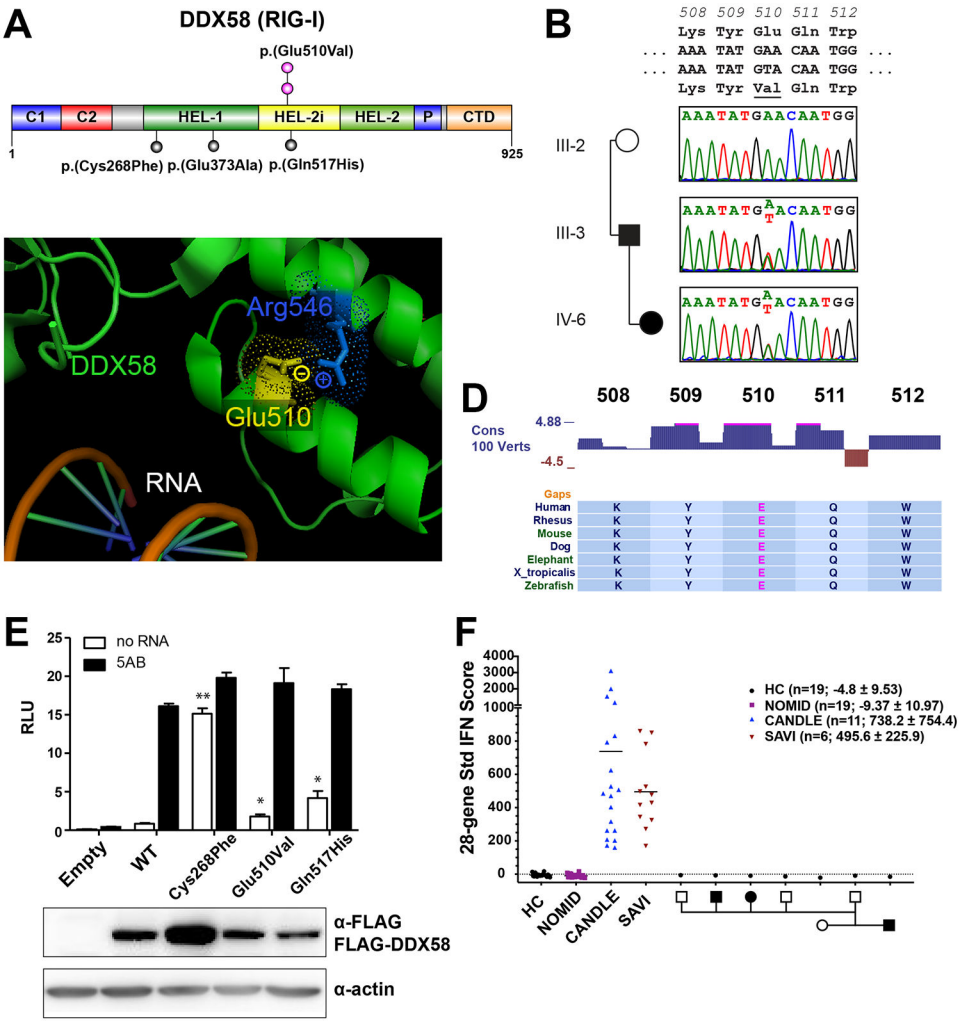


**Figure 4.**

Genetic and functional analysis of SGMRT2 families. (A) DDX58 (RIG-I) gene diagram showing location of p.(Glu510Val) variant (pink) and previously identified missense variants. (B) Sequencing chromatograms showing segregation of c.1529A>T variant in Family A. (C) Structural modeling of DDX58 bound to RNA based on crystal structure 2ykg showing charge-charge interaction of Glu510 with neighboring Arg546. (D) MultiZ 100 vertebrate conservation showing that Glu510 is an invariant residue in multiple species. Functional analysis of DDX58 p.(Glu510Val) variant. (E) Dual luciferase reporter assay with interferon-responsive element in HEK293T cells with wild-type and variant DDX58 in the presence or absence of 5AB dsRNA. *DDX58* p.(Glu510Val) variant shows significant basal activation in the absence of the RNA ligand, as do previous SGMRT2 associated variants p.(Cys268Phe) and p.(Gln517His). (F) Standardized interferon gene signature from blood for Family A members. Interferon signature is compared with autoinflammatory conditions without (i.e., NOMID - Neonatal onset multisystem inflammatory disease) and with (i.e., CANDLE - Chronic Atypical Neutrophilic Dermatosis with Lipodystrophy and Elevated temperature and SAVI - STING-associated vasculopathy with onset in infancy) an

interferon response. C, CARD domain; HEL, helicase domain; P, P-loop NTPase domain; CTD, C-terminal domain, HC, healthy control. * $p<0.05$, ** $p<0.01$.

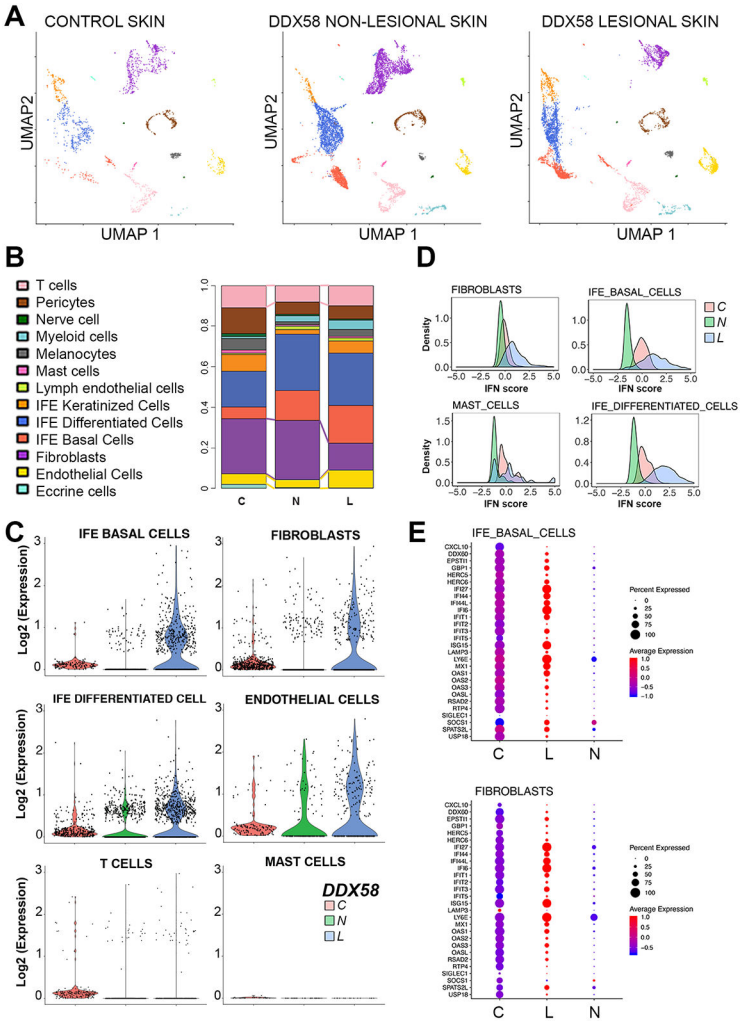


**Figure 5.**

Single cell RNA-sequencing from non-lesional and lesional skin from the index case. (A) UMAP clustering and cell populations in healthy control, non-lesional, and lesional skin from DDX58 p.(Glu510Val) variant index case. (B) Comparison of cell type proportions in control (C), non-lesional (NL) and lesional (L) skin. (C) DDX58 expression in the basal and differentiated compartments of the interfollicular epithelium (IFE); T cells; fibroblasts; endothelial cells; and mast cells. (D) Interferon responses shown as a composite “Interferon score” for different cell-types, showing increased interferon response in lesional skin (L, blue) compared to healthy controls (C, red) or non-lesional skin (NL, green). (E) Expression of individual interferon response genes in control, lesional and non-lesional basal layer keratinocytes (IFE_Basal_Cells) and fibroblasts. Circle size denotes percentage of cells showing expression, and color indicates expression levels.

**Table 1:**

Ocular and systemic features of DDX58 - Singleton Merten Syndrome Type 2 (SGMRT2) patients in this study

| | A: IV-2 | A: IV-6 | A: III-3 | B: III-1 | B: III-2 | Total n/N (%) | Total n (%) reported *DDX58*-associated SGMRT[3,4] | Total n (%) reported *IFIH1*-associated SGMRT[2,5,24] |
|---|---|---|---|---|---|---|---|---|
| **Gender** | M | F | M | M | F | | | |
| **Age** | 19 | 11 | 50 | 32 (deceased) | 36 | | | |
| **Glaucoma/ severe OHTN** | + | + | + | + | + | 5/5 (100%) | 12/13 (92%) | 6/15 (40%) |
| **Corneal transplant failure** | NA | NA | + | + | **NA** | 2/2 (100%) | NA | NA |
| **Corneal surgeries** | – | – | PKPx3 OD, DSAEK OD | PKPx6 OD, PKPx4 OS | – | | | |
| **Age at glaucoma diagnosis** | 14 | 3 | 3 | 5 | 8 | | | |
| **Visual acuity (logMAR, right/left)** | 0/0 | 0/0 | 0.6/LP | 0.8/NLP | 1.0/CF | | | |
| **Tmax (mmHg, right/left)** | 48/39 | 30/36 | NA/NA | 38/38 | 19/34 | | | |
| **IOP at last exam (mmHg, right/left)** | 15/15 | 15/14 | 7/10 | 12/Hypotony-Phthisis | 14/5 | | | |
| **Glaucoma surgery** | trabeculotomy OD, BV350 OS | 360 trabeculotomy OU | trabeculectomy OU x 2 w/ bleb needling x2 OD, goniotomy OU | trabeculectomy 3x OD, 2x OS, Ahmed OS, CTLC 2x OD and 3x OS | trabeculectomy 2x OU | | | |
| **# Glaucoma drops (right, left)** | 4/2 | 0/0 | 0/0 | 0/0 | 0/0 | | | |
| **Aortic/ valvular calcification** | – | – | + | + | – | 2/5 (40%) | 7/9 (78%) | 12/15 (80%) |
| **Cardiac arrhythmia** | – | – | – | +* | PVCs | 2/5 (40%) | 1/13 (8%) | 6/11 (55%) |
| **Acro-osteolysis of phalanx** | – | – | – | – | – | 0/5 (0%) | 8/10 (80%) | 11/14 (79%) |
| **Psoriasiform rash** | – | – | + | + | – | 2/5 (40%) | 9/13 (69%) | 11/14 (79%) |
| **Short stature** | – | – | – | – | – | 0/5 (0%) | 2/13 (15%) | 6/9 (67%) |
| **Dental anomalies** | – | – | – | + | – | 1/5 (20%) | 2/13 (15%) | 13/16 (81%) |
| **Delayed secondary dentition** | – | + | + | – | – | 2/5 (40%) | 1/2 (50%) | 8/13 (62%) |
| **Joint subluxation** | + | – | – | – | – | 1/5 (20%) | 3/13 (23%) | 12/14 (89%) |

| | A: IV-2 | A: IV-6 | A: III-3 | B: III-1 | B: III-2 | Total n/N (%) | Total n (%) reported *DDX58*-associated SGMRT[3,4] | Total n (%) reported *IFIH1*-associated SGMRT[2,5,24] |
|---|---|---|---|---|---|---|---|---|
| **Tendon rupture** | – | – | + (Achilles) | + (Achilles) | – | 2/5 (40%) | 2/13 (15%) | 7/16 (55%) |
| **Scoliosis** | – | – | – | – | – | 0/5 (0%) | 0/13 (0%) | 3/10 (30%) |
| **Dysplastic/ hypopl astic nails** | – | – | – | + | – | 1/5 (20%) | 2/13 (15%) | NA |

OHTN, ocular hypertension; PKP, penetrating keratoplasty; DSAEK, Descemet's stripping endothelial keratoplasty; logMAR, log of minimum angle of resolution; LP light perception; NLP, no light perception; CF, counting fingers; IOP, intraocular pressure; CTLC, contact transcleral laser cyclophotocoagulation; OS, left; OD, right; NA, information not available; PVC, premature ventricular contractions

*arrhythmia documented in health record, but not observed in available electrocardiograms on record.